# Studying metal impurities ($Mn^{2+}$, $Cu^{2+}$, $Fe^{3+}$) in calcium phosphates by electron paramagnetic resonance

**K. Iskhakova[1,*], F. Murzakhanov[1], G. Mamin[1], V. Putlyaev[2], E. Klimashina[2], I. Fadeeva[3], A. Fomin[3], S. Barinov[3], A. Maltsev[3], S. Bakhteev[4], R. Yusupov[4], M. Gafurov[1], and S. Orlinskii[1]**

[1]Kazan Federal University, 18 Kremlevskaya Str., Kazan, Russia
[2]Lomonosov Moscow State University, GSP-1, Leninskie Gory, Moscow, Russia
[3]Baikov Institute of Metallurgy and Materials Science, 49 Leninskii Pr., Moscow, Russia
[4]Kazan National Research Technological University, 41 K. Marxa Str., Kazan, Russia

* E-mail: kamilaiskh@gmail.com

**Abstract** Calcium phosphates (CaP) are exploited in many fields of science, including geology, chemistry, biology and medicine due to their abundance in the nature and presence in the living organism. Various analytical and biochemical methods are used for controlling their chemical content, structure, morphology, etc. Unfortunately, magnetic resonance techniques are usually not even considered as necessary tools for CaP inspection. Some aspects of application of the commercially realized electron paramagnetic resonance (EPR) approaches for characterization of CaP powders and ceramics (including the nanosized materails) such as hydroxyapatite and tricalcium phosphates of biogenic and synthetic origins containing intrinsic impurities or intentional dopants are demonstrated. The key features and advantages of the EPR techniques for CaP based materials characterization that could compliment the data obtained with the recognized analytical methods are pointed out.

## 1. Introduction

Calcium phosphates (CaP) are interesting compounds in many fields of science, including geology, chemistry, biology and medicine due to their abundance in the nature and presence in the living organism. In nature, different calcium phosphate minerals are produced within a wide range of environments by geological (igneous apatite), geochemical and/or geomicrobiological (phosphorite), and biological (biological apatite) processes. Igneous apatite minerals nucleate and crystallize from molten, phosphate-rich rock, forming crystalline fluorapatite ($Ca_5[PO_4]_3F$), chlorapatite ($Ca_5[PO_4]_3Cl$), or hydroxyapatite ($Ca_{10}[PO_4]_6[OH]_2$, HA or HAp) [1-4].

Manganese, copper and iron are essential impurity elements in CaP. Oil containing formation – rock, sands or bitumen very often possess impurity manganese and iron [5]. It is worth noting that quantitative determination of copper, manganese and iron in calcified materials is still a challenge for the analytical tools because of the structural and chemical complexity of the investigated matrix. One of the established experimental methods for identification of these ions in different types of materials (including apatites) and characterization of structure of their complexes is electron paramagnetic resonance (EPR) [6-23].

CaP materials with different functional features such as biocompatibility, catalytic activity, ion conductivity may be formed by the cation or/and anion substitution within initial matrix. For example, the experimental results indicate that HAp/$MnO_2$ composite may be an effective adsorbent for the removal of lead ions from aqueous solutions [24], while the HAp supported manganese could serve as precursor for the oxide catalysts [25]. One more characteristic was established recently for the lanthanide modified CaP – pigmentation [26, 27], that make this substances promising to be used for the development of bioactive materials for bone regeneration and smart fluorescent probes for bio imaging applications.

A huge number of publications were and are devoted to the cationic and anionic substitutions in the HAp structure while the second most frequent CaP - tricalcium phosphate (TCP) mainly in its β-form (β-TCP), is studied much less then HAp (see [28] and references therein). Despite the large number of the studies performed, many important problems relating to anionic and cationic substitutions in HAp are not sufficiently investigated. Moreover, data of different studies are contradictive. The most contradictive information is associated with the sites of the ions localization in biomineral, synthetic and nanosized samples.

Though even conventional X-band (microwave frequency of about 9 GHz) EPR is a sensitive tool for the CaP characterization, it is still not widely applied for these purpose and mainly restricted by the investigation of the radiation induced oxygen and carbonate radicals. One of the aims of the manuscript is to present some useful applications of the conventional X-band EPR and to show some abilities of the "unconventional" EPR techniques to encourage the CaP specialists to use different EPR approaches.

## 2. Materials and methods

Pure HAp, TCP and their substituted powders were obtained using a precipitation technique [29] according to the following reaction:

$$(3\text{-}x)Ca(NO_3)_2+xM(NO_3)_2+2(NH_4)_2HPO_4 \rightarrow Ca_{3-x}M_x(PO_4)_2, \quad (1)$$

where M= $Cu^{2+}$, $Fe^{3+}$, $Mn^{2+}$, x= 0;0,01; 0.05; 0.1 or 1.0. (For HAp the reaction scheme was the similar).

Synthesis procedure was as follows: the 0.5 mol/L solution of $Ca(NO_3)_2$ were mixed with a calculated amount of metal nitrate solution; then $(NH_4)_2HPO_4$ solution was added dropwise with the rate of 20 mL/min. The pH level was kept at 6.5-6.9 by the dropwise addition of ammonia solution. After 30 min, the precipitate was filtered, washed with distilled water and dried at 80°C. The precipitate was calcined at 900°C in order to remove the traces of $NH_4NO_3$ and to form the whitlockite structure.

The samples were characterized by infrared spectroscopy (Nikolet Avatar 330), atomic emission spectroscopy with inductively coupled plasma (Bruker Ultima-2), X-ray difractometry (Shimadzu 6000, Bruker D8 Advance, Rigaku D/Max-2500), X-ray fluorescence analysis with total external reflection (S2 Picofox, Bruker).

The biogenic CaP containing samples were obtained during carotid endarterectomy in patients with atherosclerosis (the inner lining of the carotid artery specimens). We investigated 27 endarterectomy specimens (plaques or fragments of plaques) derived from 27 male patients with a mean age of 57 years (42 to 64) of whom 19 were symptomatic. Based on the modified Gray-Weale classification of atherosclerotic plaques, 21 plaques were classified as "unstable" (echolucent, low median gray level, GSM ≤ 25) while 6 as "stable" (echogenic, GSM > 25). For EPR studies the tissue specimens were transferred and kept in liquid nitrogen (T = 77 K), then freeze-dried (lyophilized) at P = $5 \cdot 10^{-5}$mBar and T = 253 K (- 20°C). More details are given in paper [16].

EPR measurements were done by using W-band (with the microwave frequency of about 93.5 GHz) Bruker Elexsys 680 spectrometer and X-band (frequency of about 9.5 GHz) Bruker Elexsys 580 and table-top Labrador (Ekaterinburg, Russia).

## 3. Results and Discussion

### 3.1. Conventional EPR

Pure HA and TCP are EPR silent. Consequently, EPR can be used for the purity check and quantitative analysis of the doped CaP materials. One of the EPR features (in addition to the fact that it is a non-destructive method) is the high selective sensitivity to the complexes of the paramagnetic complexes of Mn, Fe and Cu (Figures 1, 2, 3). Though the increase of PC amount is followed by the raise of signal intensity, due to the electron spin-spin interaction the high concentrations of dopants could lead to the broadening of EPR lines and hinders the unambiguous interpretation of EPR spectra. For example, EPR pattern of HA+1 % $Mn^{2+}$ resembles that for 0.01 % of iron (cf. Figures 1 and 2).

Another remarkable feature is the sensitivity of EPR parameters to the interaction of PC with the magnetic moments of the own and neighbouring nuclei (hyperfine and super-hyperfine interaction). Because the nuclear spin I = 5/2 for $^{55}Mn$, six lines (2I + 1 = 6) of hyperfine (HF) structure for $Mn^{2+}$ with the nearly isotropic HF constant $A_{iso} \approx$ (9-10) mT is to obtain (Figures 1 and 4).

In case of even slight anisotropy of magnetic interaction tensors (such as g- and hyperfine A tensors), EPR can provide the information about their orientation dependencies and thereby about the spatial structure of the paramagnetic complexes in disordered systems. For copper both stable isotopes $^{63}Cu$ and $^{65}Cu$ have I = 3/2 and close magnetic moments. This and the known anisotropies of the spectroscopic parameters g and A for $Cu^{2+}$ in different matrices directly allow to assign presented in Figure 3 spectra to $Cu^{2+}$ due to 4 lines detected at $g_z \approx 2.4$ with $A_z \approx$ 200-250MHz.

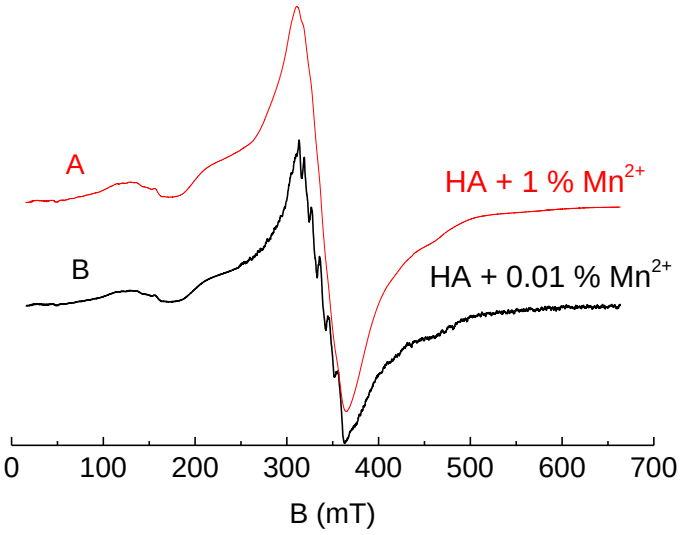


**Figure 1.** Comparison of EPR spectra of the manganese doped HAp at 9 GHz and T = 300 K for (A) 1% and (B) 0.01 % concentrations. Six lines of the hyperfine structure due to the I = 5/2 for $^{55}Mn$ nuclei is to observe for 0.01% $Mn^{2+}$. The signal amplitude (vertical axis) for 1 % $Mn^{2+}$ is reduced in 100 times.

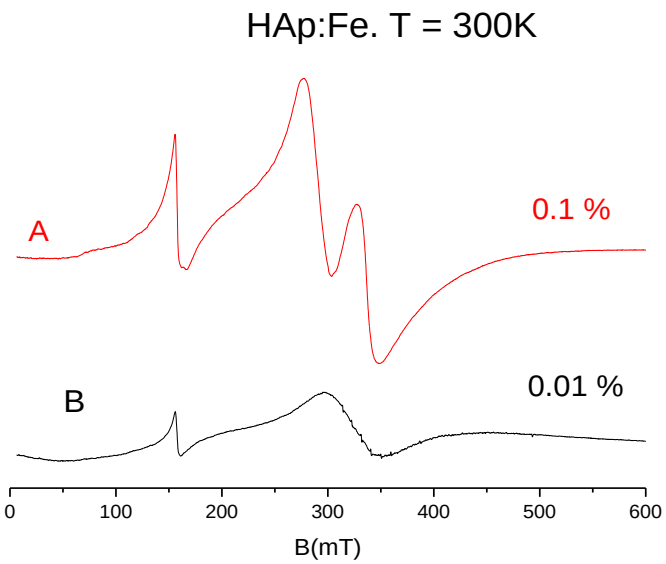


**Figure 2.** Comparison of of EPR spectra of Fe doped HA at 9 GHz and T = 300 K for (A) 0.1% and (B) 0.01% concentrations. Signals et (100-160) mT indicate that iron at least partially is in $Fe^{3+}$ state.

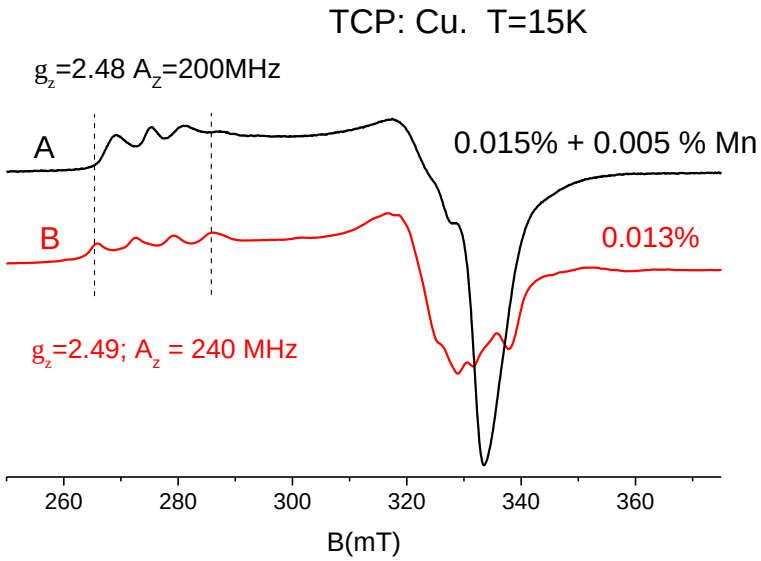


**Figure 3.** Comparison of EPR spectra of Cu doped β-TCP at 9 GHz and T = 15 K. During the synthesis, one sample (upper curve A) was co-doped with a small amount of manganese that slightly changed the EPR pattern, values of g- components and hyperfine ($A_z$) splitting compared to the "pure" Cu-doped TCP (curve B). The concentration of paramagnetic centers was derived after the double integration of EPR spectra compared to the reference one with the known concentrations. Vertical dashed lines are drawn to show the difference visually.

### 3.2. High-field and pulse EPR

Sometimes observation and interpretation of the HF structure (HFS) and superhyperfine structure (SHS) is a rather complicated task. Even in the perfect crystals the resolution of the SHS spectra, the number of the components of the structure, their relative intensities strongly depend on the concentration of PC, orientation of the applied magnetic field and the EPR frequency [30]. That is why, for example, the resolved HFS of $Mn^{2+}$ or HFS for $Cu^{2+}$ ions in the (*x*, *y*) plane (corresponding to the perpendicular orientation of B to the main axes of g-tensor) is rarely observed at X-band in the disordered systems (powders, ceramics, nanosized samples, inhomogeneous samples of biogenic origin, samples containing non-crystal amorphous phase, etc) and a transition to the higher frequencies are necessary to interpret the EPR spectra correctly (Figure 4).

Pulse methods are able to significantly increase and supplement information obtained from conventional EPR spectra. While stationary method uses continuous microwave irradiation and reveals splitting of energy levels of paramagnetic system, pulse techniques provide insights into the dynamics of the system and allows to measure relaxation times, decode complex EPR spectra of several interacting PC, etc. Because the electronic relaxation times (longitudinal or spin-lattice relaxation time $T_{1e}$ and transverse or spin-spin relaxation time $T_{2e}$) are of 3-6 orders of magnitude shorter than the nuclear ones, the characteristic time parameters are also much shorter than in nuclear magnetic resonance (NMR) experiments. The connected with those technical difficulties of creating short powerful high frequency pulses prevented till recently wide applications of the pulsed EPR approaches. The typical pulse sequences we use in our research in the W-band (94 GHz) are: (1) $\pi/2 - \tau - \pi$ with the $\pi/2$ pulse duration of 32 ns and the time delay $\tau$ = 240 ns to obtain electron spin echo (ESE, Figure 4); (2) $T_{2e}$ can be studied by tracking the primary ESE amplitude with the same $\pi/2-\pi$ pulse durations while varying $\tau$ (Figure 5); (3) $T_{1e}$ can be extracted from the inversion-recovery studies by applying the $\pi - T_{delay} - \pi/2 - \tau - \pi$ pulse sequence, while $T_{delay}$ is varied.

From Figure 4 it follows that in the atherosclerotic plaques small amount (less than 0.005 %) of $Mn^{2+}$ is obtained most probably in the crystal phase of the nanosized HAp constituent. EPR spectra and relaxation characteristics (Figure 5) differ for stable and unstable plaques that can be connected with the more inhomogeneous distribution of $Mn^{2+}$ ions in the HA structure [16]. Consequently, EPR opens one more dimension in the investigations of the calcification processes.

Since recently the technique of the simultaneously co-doping of CaP by various ions and groups to achieve desired properties attracts a great attention [31, 32]. Spectral and relaxation characteristics of PC are very sensitive to the changes in the local environment and, therefore, could be used for studying co-doping effects even if the EPR spectrum of the second (or the third) codopant is not detected because of the low concentration or masking under the EPR spectra of other PC. Figure 3 illustrates that HFS of $Cu^{2+}$ ions in TCP changes with $Mn^{2+}$ addition though the $Mn^{2+}$ spectrum is blinded by $Cu^{2+}$ one. In papers [13, 14] we have observed and investigated the influence of $Mn^{2+}$ on the relaxation parameters ($T_{2e}$) of the impurity $NO_3^-/NO_3^{2-}$ group in the micro and nano-sized HAp.

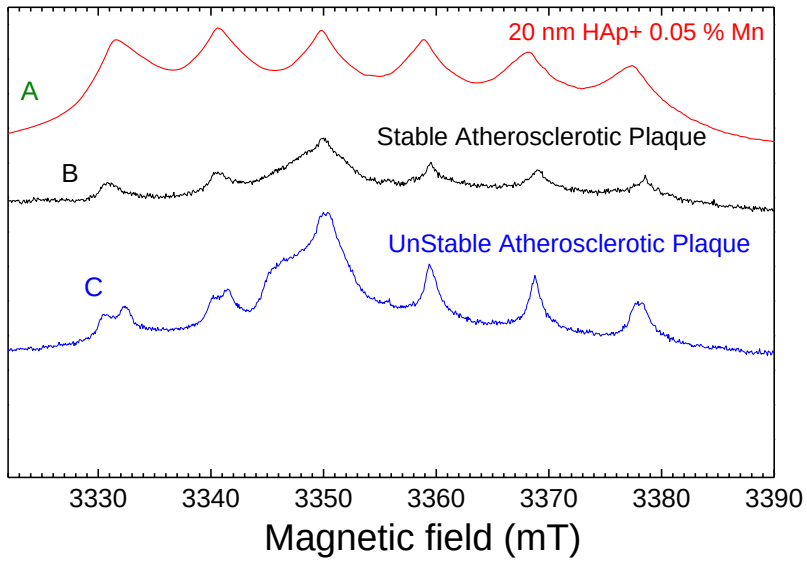


**Figure 4.** Comparison of pulsed EPR spectra at 94 GHz and T = 50 K of (A) synthetic nanohydroxyapatite with 0.05 wt % of $Mn^{2+}$; (B) stable and (C) unstable atherosclerotic plaques obtained during carotid endarterectomy in patients with atherosclerosis. Due to the small amount of samples and their inhomogeneity, the manganese spectra could not be obtained at conventional for EPR X-band (9 GHz) frequencies.

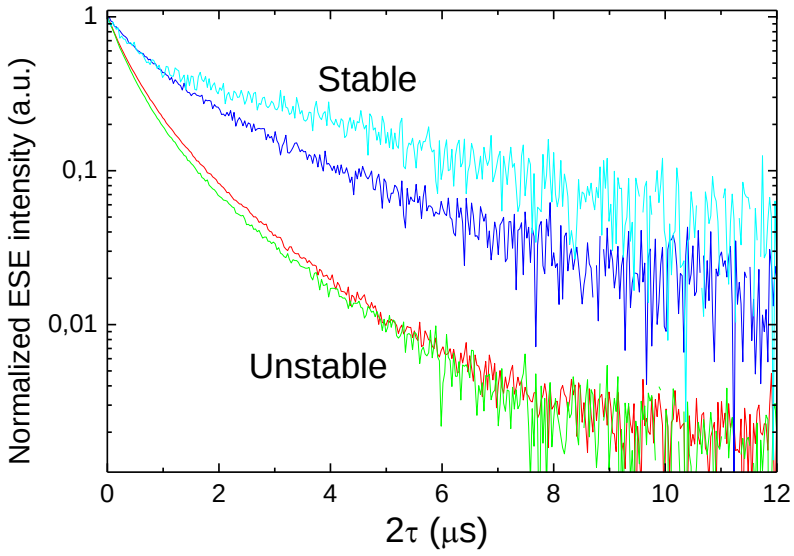


**Figure 5.** ESE decay ($T_{2e}$ curves) for $Mn^{2+}$ ions in stable (two upper curves) and unstable (two lower curves) atherosclerotic plaques taken at W-band and T = 8 K.

## 4. Conclusion

The modern commercially realized EPR techniques offer new options for the rapid testing and comprehensive examination of the condensed matter. In our opinion, the possibilities of even conventional EPR approaches for investigation and analysis of CaP materials are still not fully exploited and described in details. We hope that our paper would encourage the specialists in different scientific and industrial branches to use different EPR approaches in their studies and routine analyses.

**Acknowledgments**
The authors are thankful to T. B. Biktagirov (Kazan Federal University) for theoretical calculations. The work is financially supported by Russian Foundation for Basic Research under Grant #18-32-00337. E.K and V.P. acknowledge partial support from Lomonosov Moscow State University Program of Development,

**References**

[1] Barinov S and Komlev V 2008 Calcium phosphate based bioceramics for bone tissue enginery, , (Zurich: Trans Tech. Publ.)
[2] Omelon S, Ariganello M, Bonucci E, Grynpas M and Nanci A 2013 *Calcif. Tissue* Int. **93** 382
[3] Barinov S 2010 *Russ. Chem. Rev*. **79** 13
[4] Uskovic V and Vu V 2016 *Materials* **9** 434
[5] Khasanova N M, Gabdrakhmanov D T, Kayukova G P, Mikhaylova F N and Morozov V P 2017 *Magn. Reson. Solids* **19** 17102
[6] Low J 1957 *Phys. Rev*. **105** 793
[7] Gilinskaya L G and Sherbakova M Y 1971 *J. Struct. Chem*. **11** 950
[8] Gilinskaya L G and Sherbakova M Y 1975 *Isomorphous substitution and structural defects in apatites as found by EPR investigation* (Novosibirsk: Publishing House "Nauka") p 62 (in Russian)
[9] Mayer I, Diab H, Reinen D and Albrecht C 1993 *J. Mater. Sci*. **28** 2428
[10] Mayer I, Jacobsohn O, Niazov T, Werckmann J, Iliescu M, Richard-Plouet M, Burghaus O and Reinen D 2003 *Eur. J. Inorg. Chem*. **7** 1445
[11] Pan Y, Chen N, Weil J A and Nilges M J 2002 *Amer. Miner.* **87** 1333
[12] Pon-On W, Meejoo S and Tang I 2008 *Mater. Res. Bull.* **43** 2137
[13] Gafurov M, Biktagirov T, Mamin G, Klimashina E, Putlayev V, Kuznetsova L and Orlinskii S 2015 *Phys. Chem. Chem. Phys.* **17** 20331
[14] Gafurov M R, Biktagirov T B, Mamin G V, Shurtakova D V, Klimashina E S, Putlyaev V I and Orlinskii S B 2016 *Phys. Solid State* **58** 469
[15] Stich T A, Lahiri S, Yeagle G, Dicus M, Brynda M, Gunn A, Aznar C, DeRose V J and Britt R D 2007 *Appl. Magn. Reson*. **31** 321
[16] Chelyshev Y, Gafurov M and Ignatyev I 2016 *BioMed Res. Int.* **2016** 3706280
[17] Galukhin A V, Khelkhal M A, Gerasimov A V, Biktagirov T B, Gafurov M R, Rodionov A A and Orlinskii S B 2016 *Energy Fuels* **30** 7731
[18] Fadeeva I, Gafurov M and Kiiaeva I. 2017 *BioNanoScience* **7** 434
[19] Gafurov M, Biktagirov T, Mamin G and Orlinskii S 2014 *Appl. Magn. Reson* 45 1189
[20] Gafurov M, Biktagirov T and Yavkin B 2014 *JETP Lett.* **99** 196
[21] Biktagirov T, Gafurov M, Mamin G, Klimashina E, Putlayev V, Orlinskii S 2014 *J. Phys. Chem. A* **118** 1519
[22] Yavkin B, Mamin G and Orlinskii S. 2012 *Phys Chem Chem Phys* **14** 2246
[23] Biktagirov T, Gafurov M, Iskhakova K, Mamin G and Orlinskii S 2016 *J. Low Temp.Phys.* **185** 127
[24] Dong L, Zhu Z, Qiu Y and Zhao J 2016 *Front. Environ. Sci. Eng.* **10** 28
[25] Chlala D, Giraudon J M, Nuns N, Lancelot C, Vannier R N, Labaki M and Lamonier J F 2016 *Appl. Catal. B Environ*. **184** 87
[26] Pogosova M, Eliseev A, Kazin P and Azarmi F 2017 *Dyes and Pigments* **141** 209
[27] Kaura K, Singh K, Anand V, Islam N, Bhatia G, Kalia and Singh J 2017 *Ceram. Int.* **43** 10097
[28] Zilm M, Chen L, Sharma V, McDannald A, Jain M, Ramprasad R and Wei M 2016 *Phys. Chem. Chem. Phys.* **18** 16457
[29] Fadeeva I, Selezneva I and Davydova G 2016 *Doklady Chemistry* **468** 159
[30] Aminov L, Gafurov M, Korableva S, Kurkin I and Rodionov A 2017 *Phys.Solid State* **59** 564
[31] Kulanthaivel S, Mishra U and Agarwal T 2015 *Ceram. Int.* **41** 11323
[32] Singh R, Srivastava M, Prasad M and Kannan S 2017 J. Alloys Compd.**725** 393